

Effect of Surface Textures on the Performance Behaviours of Plain and Cycloidal Profiled Sector Shape Pad Thrust Bearings: A comparative Investigation

Shipra Aggarwal, R. K. Pandey

Abstract

Comparison of performance behaviours of fluid film thrust bearings having smooth and textured plain and cycloidal profiled sector shape pads have been presented in this paper. Surface textures on the sector shape pad have been simulated using the spherical dimples. Role of the depth, location and area density of dimples over the performance behaviours of bearing have also been investigated. Based on the analysis reported herein, it can be observed that the textured cycloidal profiled pad surfaces yield significant improvement in the performance behaviours of bearing as compared to conventional smooth plain pad. It has also been established that the surface texture introduced at certain locations on the pad surface only produces significant improvement on the performance behaviours. Moreover, surface texture present on any surface profile (plain or cycloidal) of pad yields the improvement in the performance behaviours if the values of film thickness ratio (h_1/h_2) and dimple depth ratio (d_r/h_2) fall closer to unity.

Keywords: Thrust pad bearing, cycloidal and plain profiles, surface texture, dimple, friction coefficient, load carrying capacity

1. Introduction

Surface topography of mating solids play vital role in dictating the tribological behaviours at the interface. Properly designed surfaces by providing the profiles and textures significantly improve the performance behaviours of lubricated conformal contacts [1-12]. It has been established that in the hydrodynamically lubricated thrust bearing the cycloidal surface profile on pads yields substantial improvement in the performance characteristics as compared to the conventional plain profile [2-4, 7]. Based on the literature review, it is observed that in spite of the positive results obtained with the single continuous surface profiles yet no study has been reported pertaining to exploring the improvement in the performance behaviours of thrust bearing having textured profiled pads. Therefore, the objective of this paper is to present the comparative study of the performance behaviours of plain and cycloidal profiled sector shape pad thrust bearings considering the surface textures. Mainly reduction in friction coefficient and increase in load carrying capacity of thrust bearing have been investigated and discussed herein.

2. Mathematical model

A fixed sector shape pad of hydrodynamically lubricated thrust bearing has been employed herein in the numerical analysis. Three dimensional model of thrust bearing is illustrated in Fig. 1. The coordinate system is also shown in this figure. However, the variation of film thickness in the circumferential direction for plain and

cycloidal profiles is demonstrated in Fig. 2(a). Moreover, Fig. 2(b) shows the schematic arrangement of dimples just for demonstrating a typical pattern of textured pad. However, Figs. 3(a)-(h) demonstrate the textured pads employed in the investigation.

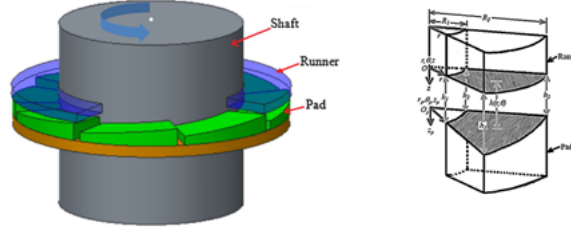


Figure 1: 3-D model of a fixed pad thrust bearing and the coordinate system used in the investigation

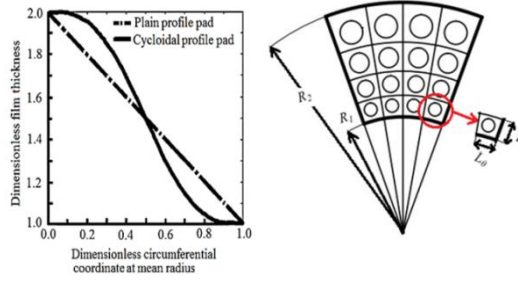


Figure 2: Plain and cycloidal profiles on pad for $h_1/h_2=2$ and illustration of a typical texture pattern on pad surface

The film thickness expressions used in the investigation are written below:

(a) For plane taper profile

$$\bar{h}_{plain} = 1 + (h_1 / h_2 - 1)(1 - \bar{\theta} / \theta_0) \quad (1)$$

(b) For cycloidal profile

$$\bar{h}_{cycloidal} = 1 + \left[(h_1 / h_2 - 1) \left(\bar{\theta} / \bar{\theta}_0 - (0.5 / \pi) \sin(2\pi \bar{\theta} / \bar{\theta}_0) \right) \right] \quad (2)$$

(c) For spherical dimples (for details refer [13])

$$\bar{h}_{dimple} = (d_{max} / (r_d h_2)) \sqrt{r_d^2 - (r\theta - r_{\theta_c})^2 - (r - r_c)^2} \quad (3)$$

where d_{max} : maximum depth of dimple, r_d : radius of dimple

(d) Plain profile with texture (spherical dimpled surface)

$$\bar{h} = \bar{h}_{plain} + \bar{h}_{dimple} \quad (4)$$

(e) Cycloidal profile with texture (spherical dimpled surface)

$$\bar{h} = \bar{h}_{cycloidal} + \bar{h}_{dimple} \quad (5)$$

The Reynolds equation incorporating the mass conservation algorithm is employed in the investigation considering the non-inertial, steady state, and laminar flow of Newtonian lubricant. This equation is expressed as follows [7, 13]:

$$\frac{1}{\bar{r}} \frac{\partial}{\partial \bar{r}} \left(g \frac{\bar{r} \bar{h}^3}{\bar{\eta}} \frac{\partial \phi}{\partial \bar{r}} \right) + \frac{1}{\bar{r}^2} \frac{\partial}{\partial \bar{\theta}} \left(g \frac{\bar{h}^3}{\bar{\eta}} \frac{\partial \phi}{\partial \bar{\theta}} \right) = \lambda \frac{\partial}{\partial \bar{\theta}} (\bar{h} \phi) \quad (6)$$

$$\text{where } \phi = \rho / \rho_c, \beta = \rho \frac{\partial p}{\partial \rho}, \lambda = \frac{6\eta_0 \Omega R_m^2}{h_2^2 \beta}, g = \begin{cases} 0 & \text{when } \phi < 1 \\ 1 & \text{when } \phi \geq 1 \end{cases}$$

$$\bar{h} = \frac{h}{h_2}, \bar{R}_1 = \frac{R_1}{R_m}, \bar{R}_2 = \frac{R_2}{R_m}, \bar{r} = \frac{r}{R_m}, \bar{\eta} = \frac{\eta}{\eta_0}, \bar{\theta} = \theta$$

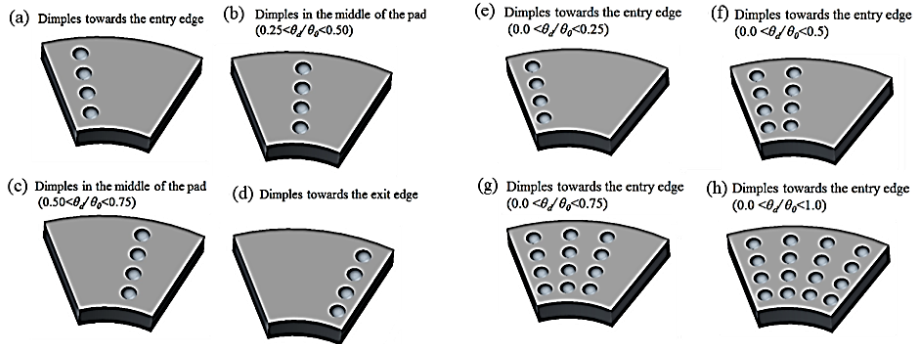


Figure 3: Demonstration of textured pad surfaces employed in the study

Equation (6) is solved for ‘ ϕ ’ for computing the pressure using the following relation [13]:

$$p = p_c + g \beta [\ln(\phi)] \quad (7)$$

The pressure values computed at the discrete nodes are used to compute the load carrying capacity using the following relation:

$$\bar{W} = \int_{\bar{R}_1}^{\bar{R}_2} \int_0^{\bar{\theta}_0} \bar{p} \bar{r} d\bar{r} d\bar{\theta} \quad (8)$$

Friction force is computed using the relation as written below:

$$\bar{F} = \int_{\bar{R}_1}^{\bar{R}_2} \int_0^{\bar{\theta}_0} [(1/\bar{h})(\partial\bar{v}_\theta / \partial\bar{z})] \bar{r} d\bar{r} d\bar{\theta} \quad (9)$$

Coefficient of friction is obtained using the following relation:

$$\mu = (\bar{F} / \bar{W})(h_2 / R_m) \quad (10)$$

3. Computational procedure

Coupled solution of governing equations is obtained using finite difference method and Gauss Seidel iterative schemes. After performing grid independence test, it has been decided generate the numerical results using 331 (N_θ) x 331 (N_r) grids. All the results have been generated using the following convergence criteria:

$$\left(\frac{\sum_{i=1}^{N_\theta} \sum_{j=1}^{N_r} |\phi(i, j)_{new} - \phi(i, j)_{old}|}{\sum_{i=1}^{N_\theta} \sum_{j=1}^{N_r} |\phi(i, j)_{new}|} \right) \leq 10^{-11} \quad (11)$$

4. Results and discussion

For developing the confidence in the results generated through the proposed model, the comparison of pressure profile has been done with the work of Huebner [14]. Good matching of pressure profiles can be seen in Fig.4. This provides the correctness of the proposed model for use in generating the numerical results. Using the input data listed in Table 1, all the numerical results reported herein have been generated. Moreover, additional data have also been provided with the presented figures.

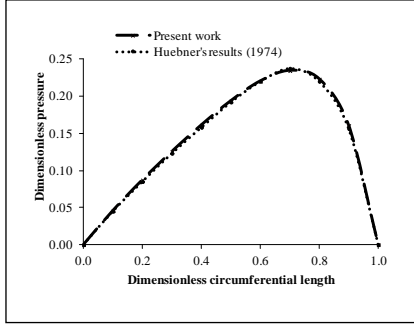
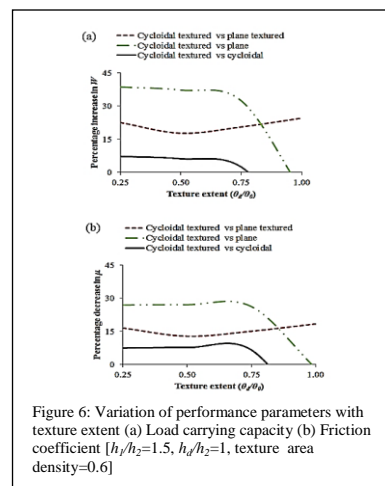
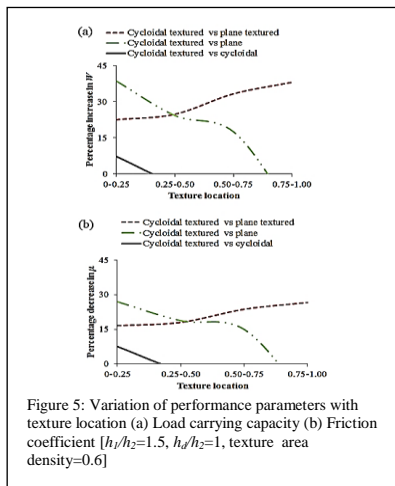


Table 1 Input data

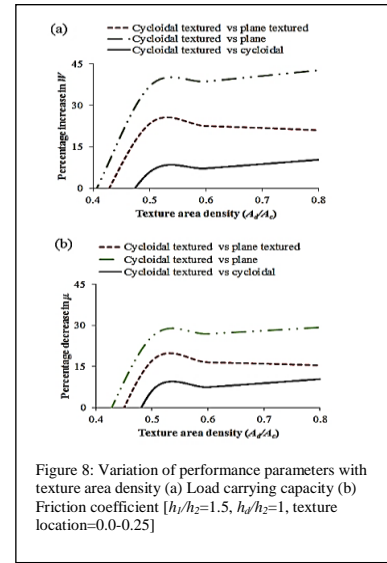
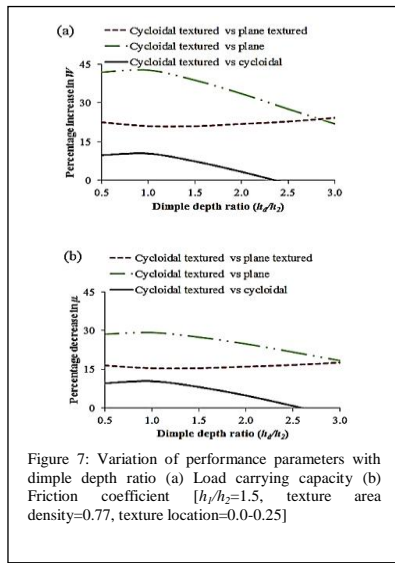
Exit film thickness (h_2), μm	38.1
Inlet film thickness (h_1), μm	$1.5h_2, 2h_2$
Inner radius of sector pad (R_1), m	0.025
Outer radius of sector pad (R_2), m	0.058
Width of the pad (b), m	0.033
Lubricant viscosity (η_0), Pa-s	0.042
Runner speed (N), rpm	5000
Pad sector angle (θ_0), Deg	45

Figure 4: Comparison of present results with work of reference [14]

The performance behaviours (increase in the load carrying capacity and reduction in friction coefficient) of the thrust bearing have been presented in Figs. 5-14 for various operating parameters. Increase in the load carrying capacity and decrease in the friction coefficient of textured cycloidal profiled pad thrust bearing have been shown in these figures with respect to (i) smooth plain pad, (ii) smooth cycloidal profiled pad, and (iii) textured plain pad. To understand the roles of texture location and its distribution on the bearing's performance parameters (load carrying capacity and friction coefficient), the comparative results have been demonstrated in the Figs. 5 and 6. It can be seen in these figures that surface texture lying toward the entry edge on the cycloidal profiled pad is beneficial. It yields about 7% increase in the load carrying capacity and 7% reduction in friction coefficient in comparison to smooth cycloidal profile pad for the texture/dimple parameters provided with the figure. Moreover with textured cycloidal profile pad, about 38% and 22% increase in the load carrying capacity are recorded in comparison to smooth plain and textured plain pads, respectively.

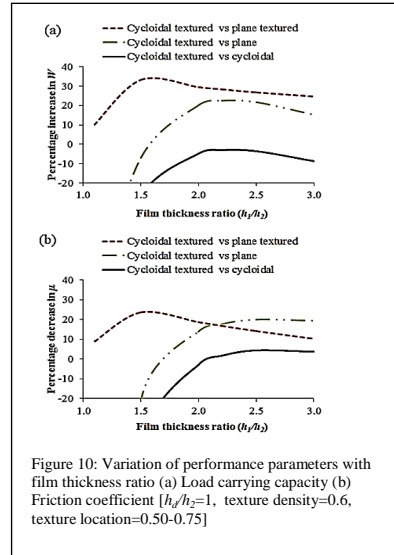
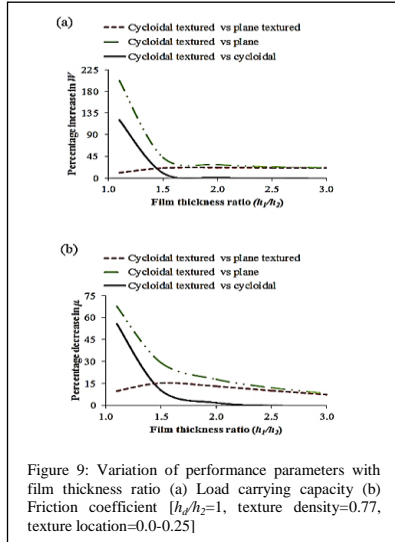


Figures 7(a) and 7(b) demonstrate the variation in the load carrying capacity and friction coefficient with the parameter ' h_d/h_2 ', respectively. With increase in ' h_d/h_2 ' value up to 1.0, the load carrying capacity first increases, thereafter it decreases. About 42% increase in load carrying capacity has been achieved with textured cycloidal profiled pad in comparison to conventional plain pad. Moreover, the effect of texture area density variation on the increase in the load carrying capacity and decrease in friction coefficient has been demonstrated in Fig. 8. It can be seen in this figure that there is increase in load carrying capacity and decrease in coefficient of friction with increase in texture area density.

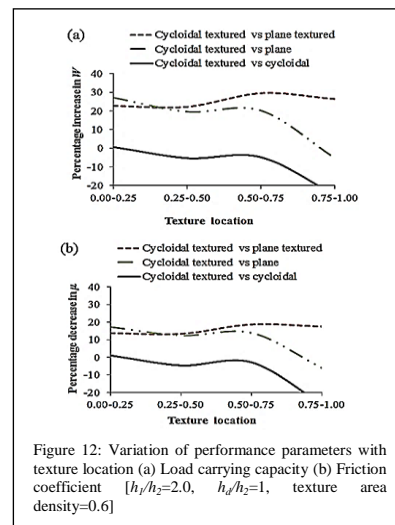
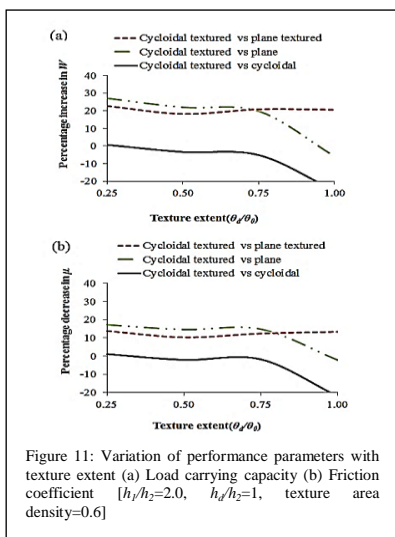


The effect of film thickness ratio variation on the increase in load carrying capacity and decrease in coefficient of friction has been presented in Figs. 9 and 10 for the location of textures lying on the pad between the normalised circumferential lengths of 0.0-0.25 and 0.50-0.75, respectively. In Fig. 9, it can be observed that as the film thickness ratio enhances both the increase in the load carrying capacity and decrease in the coefficient of friction start diminishing. This indicates that providing the dimples towards the entry edge of the pad for small values of h_1/h_2 ratio is more beneficial mainly in term of enhanced load carrying capacity. At the film thickness ratio=1.5, textured cycloidal profiled pad produces 42% increase in the load carrying capacity and 29% decrease in the friction coefficient in comparison to smooth plain pad. Performance parameters have also been computed for very low values of film thickness ratio(1.001 and 1.01). At film thickness ratio of 1.001, about 27000% increase in the load carrying capacity and 99% decrease in the coefficient of friction are obtained with textured cycloidal profiled pad in comparison to smooth plain pad. It is worth mentioning here that the film thickness ratio=1.001 can be considered between nearly parallel surfaces, thus, this type of bearing configuration sustains very small magnitude of load. It can be observed in Fig. 10 that the presence of surface texture between the normalized circumferential location 0.5-0.75 results in decrease in the load carrying capacity and increase in the friction coefficient in

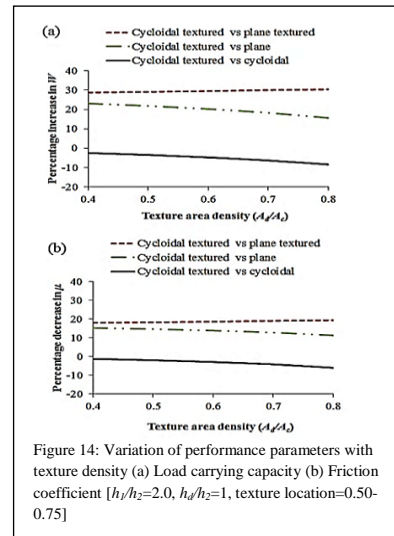
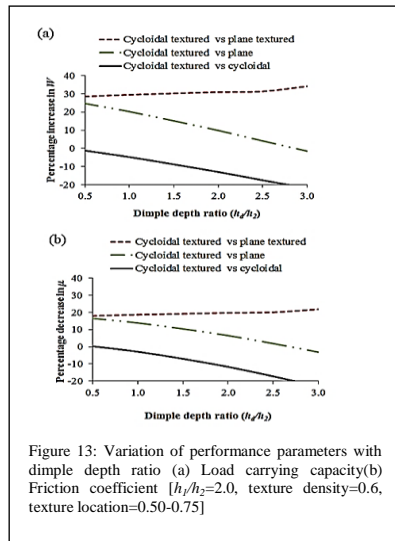
comparison to cycloidal profiled pad. Hence, presence of surface texture on pad toward the exit edge is not beneficial.



Effects of dimple depth, texture location, texture distribution and texture area density on the performance behaviour of pad thrust bearing have been explored and presented in Figs. 11-14. In Figures 11 and 12, it can be seen that the presence of texture toward the entry edge (0.0-0.25) yields in the marginal increase in the load carrying capacity and marginal decrease in coefficient of friction in comparison to cycloidal profiled pad. However, the surface texture placed at other locations results in the decrease in load carrying capacity and increase in coefficient of friction in comparison to cycloidal profiled pad.



Influence of the dimple depth and texture area density on the performance behaviour of pad thrust bearing can be seen in Figs. 13 and 14, respectively. With increase in the dimple depth the load carrying capacity decreases and coefficient of friction increases in comparison to cycloidal profiled pad. Similarly, the load carrying capacity decreases and coefficient of friction increases with increase in the texture area density.



5. Conclusions

Based on the studies reported in this paper, the following conclusions have been drawn:

- Textured surface provided on the pad toward the entry edge produces significant benefits in terms of increase in the load carrying capacity and reduction in the friction coefficient of thrust bearing. However, the texture placed at other locations on the pad surface results in deterioration of the performance parameters.
- Textured cycloidal profiled pad produces increase in load carrying capacity in comparison to cycloidal profiled pad, textured plain pad, and smooth plain pad.
- Significant improvement in load carrying capacity and reduction in friction coefficient have been obtained for low values of film thickness ratios (1.001 to 1.01). Surface texture present on any surface profile (plain or cycloidal) of pad yields the improvement in the performance behaviours if the values of dimple depth ratio (d_H/h_2) fall closer to unity.

References

- [1] I. Etsion, "State of the art in laser texturing", Transactions of the ASME, Journal of Tribology, vol. 127, pp. 248-253, 2005.

- [2] R. K. Sharma, R. K. Pandey, "Thermohydrodynamic analysis of infinitely wide cycloidal profiled pad thrust bearing with rough surface and a comparison to plane profiled pad", *Lubrication Science*, vol. 20, pp. 183-203, 2008.
- [3] R. K. Sharma, R. K. Pandey, "Influence of surface profiles on slider bearing performance", *International Journal of Surface Science and Engineering*, vol. 3/4, pp. 265-280, 2008.
- [4] R. K. Sharma, R. K. Pandey, "Experimental studies of pressure distributions in finite slider bearing with single continuous surface profiles on the pads", *Tribology International*, vol. 42, pp. 1040-1045, 2009.
- [5] R. C. Singh, R. Chaudhary, R. K. Pandey, S. Maji, "Experimental studies for the role of piston rings' face profiles on performance of a diesel engine fuelled with diesel and jatropha based biodiesel", *Journal of Scientific & Industrial Research*, vol. 71, pp.57-62, 2012.
- [6] S. Aggarwal, R. K. Pandey, "Performance behaviour of sector shape taper-flat pad thrust bearing with different taper surface profiles" *Proceedings of National Tribology Conference (NTC-2014) held during 15th-17th December 2014 at PES University, Bengaluru, India.*
- [7] S. Aggarwal, R. K. Pandey, "Combined effects of grooves and dimples on the performance parameters of sector shaped pad thrust bearing", *Proceedings of International Conference on Industrial Tribology (ICIT-2012) held during 7th-9th December 2012 at Pune, India.*
- [8] Y. Henry, J. Bouyer, M. Fillon, "An experimental analysis of the hydrodynamic contribution of textured thrust bearings during steady-state operation: a comparison with the un-textured parallel surface configuration", *Proceedings of Institution of Mechanical Engineers, Part-J, Journal of Engineering Tribology*, vol. 229, pp.362-375, 2014.
- [9] X. Shi, T. Ni, "Effects of groove textures on fully lubricated sliding with cavitation", *Tribology International*, vol. 44, pp. 2022-2028, 2011.
- [10] C. I. Papadopoulos, P. G. Nikolakopoulos, L. Kaiktsis, "Evolutionary optimization of micro-thrust bearings with periodic partial trapezoidal surface texturing", *Transactions of the ASME, Journal of Engineering for Gas Turbines and Power*, vol. 133, pp.012301-1-10, 2011.
- [11] F. M. Meng, "On influence of cavitation in lubricant upon tribological performances of textured surfaces", *Optics & Laser Technology*, vol. 48, pp. 422-431, 2013.
- [12] D. G. Fouflia, A. G. Charitopoulos, C. I. Papadopoulos, L. Kaiktsis, M. Fillon, "Performance comparison between textured, pocket, and tapered-land sector-pad thrust bearings using computational fluid dynamics thermohydrodynamic analysis", *Proceedings of Institution of Mechanical Engineers, Part-J, Journal of Engineering Tribology*, vol. 229, pp. 376-397, 2014.
- [13] S. Kango, R. K. Sharma, R. K. Pandey, "Thermal analysis of microtextured journal bearing using non-Newtonian rheology of lubricant and JFO boundary conditions", *Tribology International*, vol. 69, pp. 19-29, 2014.
- [14] K. H. Huebner, "A three dimensional thermohydrodynamic analysis of sector thrust bearing", *Transaction ASLE*, vol. 17, pp. 62-73, 1974.